RSC Advances

PAPER

View Article Online
View Journal | View Issue

Cite this: *RSC Adv.*, 2017, **7**, 29827

A highly selective fluorescent chemosensor for Fe^{3+} based on a new diarylethene with a rhodamine 6G unit†

Huitao Xu, Haichang Ding, Gang Li, Congbin Fan, Gang Liu* and Shouzhi Pu*

Received 27th April 2017
Accepted 16th May 2017

DOI: 10.1039/c7ra04728b

rsc.li/rsc-advances

Herein, a new diarylethene derivative bearing rhodamine 6G (**1O**) was synthesized *via* Schiff base condensation. It exhibited a sensitive response to Fe^{3+} with the solution changing from colorless (no fluorescence) to distinct pink (strong fluorescence) due to the transformation of the spirolactam ring to the open ring of rhodamine 6G. The diarylethene derivative bound to Fe^{3+} in the binding stoichiometry of 1 : 1, and the limit of detection (LOD) of the **1O** chemosensor for Fe^{3+} detection was found to be 65 nM. In addition, **1O** exhibited an obvious acidichromism to TFA and could function as a reversible fluorescence photoswitch in response to UV/vis light irradiation. Based on these observations, a logic circuit was constructed with the combinational stimuli of UV/vis light and Fe^{3+}/EDTA as inputs and the fluorescent emission intensity at 585 nm as the output.

Introduction

Heavy metal cations, such as Hg^{2+}, Cu^{2+}, and Fe^{3+}, naturally exist and have been widely used in many industrial fields. They are toxic at high concentrations and are responsible for many incidents of industrial and agricultural pollution.[1–3] Compared to the time-consuming and expensive instrumental techniques reported for heavy metal-ion detection, a chemosensor is a faster, cheaper, more powerful, and highly sensitive molecular tool for the detection of many biological and environmental heavy metal pollutants.[4–6] Among all chemosensors, fluorescent chemosensors have attracted significant attention due to their simple operation, high sensitivity, and real-time detection. Fe^{3+} plays a key role in many biochemical processes at the cellular level and is indispensable for most of the organisms.[7] It provides oxygen-carrying capacity to heme and acts as a cofactor in many enzymatic reactions involved in the mitochondrial respiratory chain. However, high levels of Fe^{3+} within the body can be associated with increased incidence of certain cancers and dysfunction of organs such as heart, pancreas, and liver.[8–11] Therefore, new simple and efficient chemosensors for Fe^{3+} detection are highly desired.[12] Several fluorescent sensors have been developed for Fe^{3+} detection. However, most of them detect Fe^{3+} based on fluorescence quenching by the paramagnetic property of Fe^{3+}.[13] For example, in an early study, Wolf *et al.* selectively detected Fe^{3+} in aqueous solutions with a 1,8-diacridylnaphthalene-derived fluorosensor based on fluorescence quenching. Therefore, the development of highly selective turn-on response chemosensors for Fe^{3+} is of significance and challenging.[14] Photochromic materials can be potentially applied to optical memories, photoswitches, logic circuits, and chemosensors.[15,16] Diarylethenes, one of the most promising photoresponsive compounds, have attracted significant research interests due to their excellent thermal stability, notable fatigue resistance, high sensitivity, and rapid response.[17,18]

In particular, they can function as a fluorescence sensor based on their reversible fluorescence response to UV/vis lights irradiation. Recently, many diarylethene-based sensors have been reported. Zheng *et al.* prepared a dual-control molecular switch based on photochromic hexahydrogen cyclopentene bearing two rhodamine units and demonstrated it as an integrated logic circuit at the molecular level. Pu *et al.* exploited diarylethene-based fluorescence sensors to detect Fe^{3+}, Hg^{2+}, and Cu^{2+}.[19,20] Their study has contributed towards the comprehensive understanding of the sensors based on diarylethene-bearing functional groups.

The rhodamine 6G-based fluorescent chemosensor is an excellent fluorophore for metal ion detection and has attracted extensive interest in recent years by virtue of its excellent photophysical properties such as long excitation and emission wavelength, high fluorescence quantum efficiency, and excellent detection sensitivity.[21,22] The off–on fluorescence switching of the chemosensor is based on the transformation between the spirocyclic and open ring forms of rhodamine 6G. The chemosensor is in the spirocyclic form in the absence of metal ions and exhibits no color or fluorescent emission. The addition of suitable metal ions can open the spirocycle *via* coordination, leading to chromogenic and fluorogenic responses.

Jiangxi Key Laboratory of Organic Chemistry, Jiangxi Science and Technology Normal University, Nanchang, Jiangxi 330013, PR China. E-mail: liugang0926@163.com; pushouzhi@tsinghua.org.cn; Fax: +86-791-83831996; Tel: +86-791-83831996

† Electronic supplementary information (ESI) available. See DOI: 10.1039/c7ra04728b

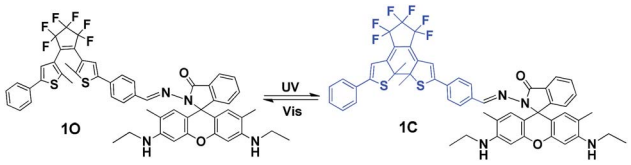

Scheme 1 Photochromism of diarylethene **1O**.

In the present study, a diarylethene derivative bearing a rhodamine 6G moiety was synthesized to construct a fluorescent chemosensor for Fe^{3+} detection. The chemosensor exhibited excellent selectivity and sensitivity for Fe^{3+} detection *via* the turn on fluorescence signal in an aqueous acetonitrile solution (v/v = 1 : 1). Scheme 1 is the schematic of the photochromism of the diarylethene derivative.

Experimental

General methods

Chemical reagents were obtained from J & K Scientific Ltd and were used as received. All the reagents and solvents were of analytical grade and diluted as required. All cations were added in the form of metal nitrates except for K^+, Ba^{2+}, Mn^{2+}, and Hg^{2+} that were added as metal chlorides. The stock solutions of the metal ions were prepared in distilled water at the concentration of 0.1 mol L^{-1}.

NMR spectra were obtained using a Bruker AV400 (400 MHz) spectrometer with $CDCl_3$ and DMSO-d_6 as the solvents and tetramethylsilane (TMS) as the internal standard. Fluorescence quantum yield was measured using an Absolute PL Quantum Yield Spectrometer QY C11347-11. UV/vis spectra were obtained using an Agilent 8453 UV/vis spectrophotometer. The fluorescence spectra were obtained *via* a Hitachi F-4600 fluorescence spectrophotometer. Infrared spectra (IR) were obtained using a Bruker Vertex-70 FT-IR spectrometer.

Synthesis of 1O

Scheme 2 shows the synthesis route of the target compound, [1-(2-methyl-5-phenyl-3-thienyl)-2-{2-methyl-5-[4-*N*(rhodamine-6G)-hydrazide]phenyl-3-thienyl}perfluorocyclopentene] (**1O**). 3-Bromo-2-methyl-5-(1,3-dioxolane)thiophene (**3**), (2-methyl-5-phenyl-3-thieryl)perfluorocyclopentene (**4**), and **8** were synthesized as described in the literature.[23–27] Compound **3** was coupled with **4** to afford compound **5**, which was hydrolyzed to produce compound **6**. Compound **8** reacted with **6** in anhydrous ethanol *via* Schiff base condensation to afford the target compound **1O**. The detailed procedure is described as follows.

A solution of *n*-BuLi/hexane (2.5 mol L^{-1}, 4.90 mL) was added dropwise to 60 mL of compound **3** (3.24 g, 10.00 mmol) solution in anhydrous THF at 195 K under stirring and an argon atmosphere and stirred for 30 min. Compound **4** (3.67 g, 10.00 mmol) was slowly added to the reaction mixture at 195 K, further stirred for 3 h at the same temperature, and quenched with water. The product was extracted with dichloromethane, dried over Na_2SO_4, filtered, and evaporated. The crude product was purified by column chromatography using the petroleum ether–ethyl acetate (v/v = 10 : 1) as the eluent to afford the compound **5** (2.60 g, 4.40 mmol), which was refluxed in acetone–water (v/v = 4 : 1) for 2 h, extracted with dichloromethane, dried over Na_2SO_4, filtered, evaporated, and purified by column chromatography to afford compound **6** as a blue solid with a yield of 84%. Mp: 363–365 K. ^{1}H NMR ($CDCl_3$, 400 MHz), δ (ppm): 1.90 (t, 3H, J = 8.0 Hz), 1.93 (s, 3H), 7.21 (s, 1H), 7.25 (d, 1H, J = 8.0 Hz), 7.32 (t, 2H, J = 8.0 Hz), 7.37 (s, 1H), 7.47 (d, 2H, J = 8.0 Hz), 7.63 (d, 2H, J = 8.0 Hz), 7.83 (d, 2H, J = 8.0 Hz), 9.94 (s, 1H).

A solution of compound **8** (0.98 g, 0.20 mmol) in 15 mL anhydrous ethanol was added to a solution of compound **6** (0.11 g, 0.20 mmol) under constant stirring, refluxed for 48 h, cooled down to room temperature, and quenched with water. The solvent was removed under reduced pressure. The residue was extracted with dichloromethane, and the organic phase was dried over Na_2SO_4, filtered, and evaporated. The crude product was purified by column chromatography on a silica gel column using petroleum ether–ethyl acetate (v/v = 4 : 1) as the eluent to afford **1O** (0.10 g, 0.10 mmol) as a light purple solid in 51% yield. Mp: 430–432 K. ^{1}H NMR (DMSO-d_6, 400 MHz), δ (ppm) 1.19 (t, 6H, J = 8.0 Hz), 1.82 (s, 6H), 1.96 (s, 6H), 3.10–3.13 (m, 4H), 5.05 (s, 2H), 6.16 (s, 2H), 6.32 (s, 2H), 7.03 (d, 1H, J = 8.0 Hz), 7.33 (d, 1H, J = 8.0 Hz), 7.41 (d, 3H, J = 4.0 Hz), 7.47 (s, 1H), 7.51 (s, 1H), 7.55–7.60 (m, 6H), 7.73 (s, 1H) 7.90 (d, 1H, J = 8.0 Hz), 8.64 (s, 1H) (Fig. S1†). ^{13}C NMR (DMSO-d_6, 100 MHz), δ (ppm): 13.97, 14.08, 16.86, 37.40, 62.73, 65.56, 95.67, 104.95, 118.15, 122.48, 122.92, 123.19, 123.72, 125.21, 125.48, 126.78, 127.37, 128.05, 128.10, 128.63, 128.80, 129.13, 132.42, 133.78, 134.08, 140.85, 141.13, 141.65, 141.83, 145.75, 147.74, 150.94, 151.29, 163.69

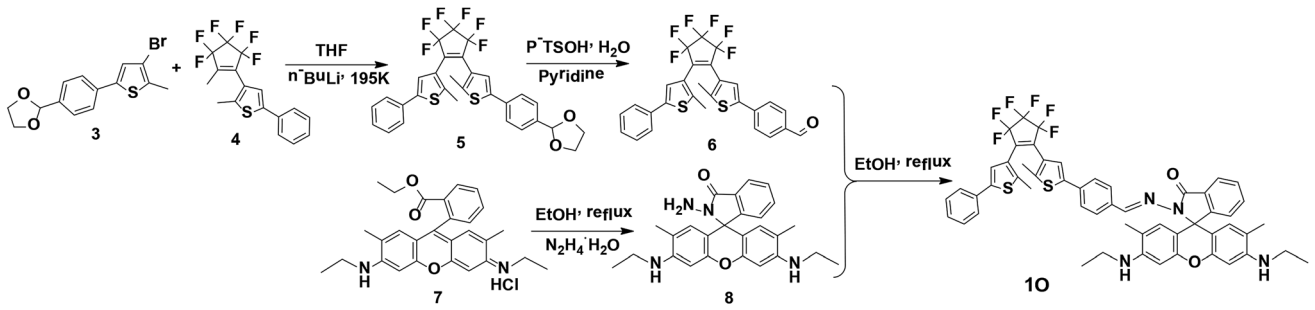

Scheme 2 Synthesis route for diarylethene **1O**.

(Fig. S2†). MS (*m*/*z*): 959.28 $[M + H]^+$ (Fig. S3†); IR (KBr, ν, cm^{-1}): 1199, 1216, 1267, 1315, 1515, 1608, 1620, 1636, 1684, 1713.

Results and discussion

Photochromism of 1O

The photochromic properties of **1O** were determined in acetonitrile ($C = 2 \times 10^{-5}$ mol L^{-1}) at room temperature. The open ring isomer **1O** exhibited an absorption peak at 353 nm (Fig. 1A) due to the π^*–π transition.[28] A new absorption band centered at 602 nm appeared, and the solution of **1O** turned from colorless to blue under the irradiation at 297 nm, indicating that the closed-ring form **1C** was formed. The blue solution of **1C** could be bleached to colorless under the visible light irradiation at $\lambda >$ 500 nm, and its absorption peak shifted back to 353 nm. An isosbestic point appeared at 370 nm, indicating that a two-component photochromic reaction occured.[29–31] The cyclization and cycloreversion quantum yields of **1O** were determined to be 0.232 and 0.003, respectively, with 1,2-bis(2-methyl-5-phenyl-3-thienyl)perfluorocyclopentene as a ref. 32 The fatigue resistance of **1O** revealed that **1O** degraded only 8.3% after 10 coloration–discoloration cycles in response to the alternate irradiations of UV/vis lights at room temperature (Fig. 1B).

Spectral response of 1O to Fe^{3+}

It has been reported that rhodamine 6G derivatives are subject to significant changes in absorption or fluorescence spectra upon coordination with metal ions and thus can be used as a sensitive probe for metal ion detection.[33] In the present study, the fluorescence of **1O** ($C = 2.0 \times 10^{-5}$ mol L^{-1}) induced by metal ions including Fe^{3+}, Cr^{3+}, Al^{3+}, Hg^{2+}, Cu^{2+}, Mg^{2+}, Ba^{2+}, Zn^{2+}, Mn^{2+}, Co^{2+}, Ni^{2+}, Ca^{2+}, Cd^{2+}, Pb^{2+}, Sr^{2+}, and K^+ was determined in an aqueous acetonitrile solution (v/v = 1 : 1) at room temperature. As shown in Fig. 2A, for the absorption spectra of **1O** in the presence of 10.0 equiv. of metal ions, only Fe^{3+}, Cr^{3+}, and Al^{3+} were able to induce strong absorptions at 531 nm, and Fe^{3+} caused a much stronger absorption peak than Cr^{3+} and Al^{3+}.

Compound **1O** in acetonitrile exhibited no obvious emission signal under excitation at 515 nm. The addition of 10.0 equiv. of Fe^{3+} to the **1O** solution led to *ca.* 168-fold increase in the fluorescent emission intensity at 585 nm (Fig. 2B). The **1O** solution showed weaker responses to Cr^{3+} and Al^{3+} with 45-fold and 28-fold increases in fluorescent emission peaks at 578 nm and 585 nm, respectively (Fig. S4†). These observations indicate that **1O** can be potentially used as a selective fluorescence sensor for Fe^{3+} in an acetonitrile/water binary solvent system (v/v = 1 : 1). In addition, Fe^{3+} turned the **1O** solution from colorless to pink and from dark to a bright green yellow color under excitation at 515 nm due to the formation of the open ring amide form of rhodamine 6G (**1O′**) (Fig. 2C). Other metal ions caused no detectable increase in the emission intensity or solution color of **1O** in the aqueous acetonitrile solution except for Cr^{3+}, Al^{3+}, and Cu^{2+} that turned the **1O** solution to pale pink and caused a weak fluorescent emission (Fig. 2C).

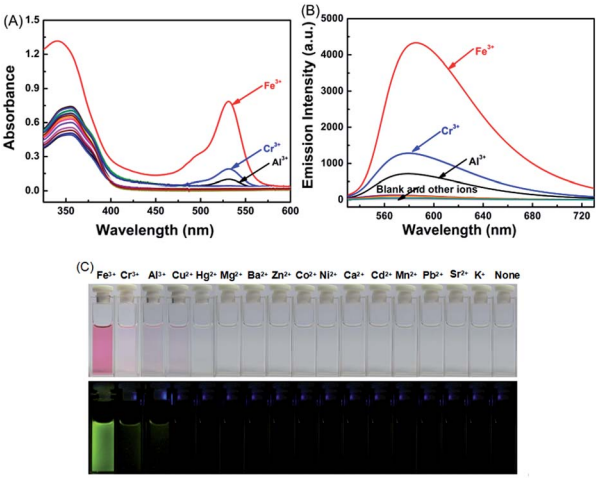

Fig. 2 Changes in fluorescence of **1O** in response to various metal ions (10.0 equiv.) in aqueous acetonitrile solution ($C = 2.0 \times 10^{-5}$ mol L^{-1}, v/v = 1 : 1). (A) Absorption spectral changes. (B) Changes in fluorescence. (C) Color and fluorescence changes of **1O** after the addition of 10.0 equiv. of different metal ions.

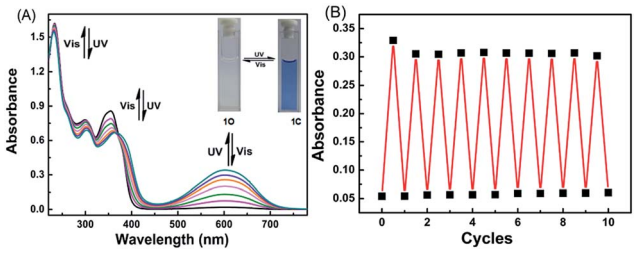

Fig. 1 (A) Changes in the absorption spectra of diarylethene **1O** in acetonitrile ($C = 2.0 \times 10^{-5}$ mol L^{-1}) at room temperature. (B) Fatigue resistance of **1O** in acetonitrile ($C = 2.0 \times 10^{-5}$ mol L^{-1}) at room temperature.

The chemosensing properties of **1O** towards Fe^{3+} were further investigated *via* absorption and fluorescence titration. As shown in Fig. 3, the solution of **1O** changed from colorless to pink (Fig. 3A), and a new absorption band centered at 530 nm appeared with the increase of Fe^{3+} equiv. from 0 to 10.0 due to the formation of **1O′** (Fig. 3B). Further increase in the Fe^{3+} amount caused no significant change in the absorption of **1O**. Moreover, the fluorescent emission of **1O** at 585 under excitation at 515 nm increased with the increase of Fe^{3+} equiv and peaked at 10.0 equiv. (Fig. 3C). The absolute fluorescence quantum yield was determined to be 0.43. The fluorescence intensity changes with the addition of Fe^{3+} were also visibly observed with the naked eye, with the solution turning from dark to a bright green-yellow under excitation at 515 nm (Fig. 3D).

The fluorescence was reverted by addition of an excess of EDTA (10.0 equiv.), indicating that the coordination of **1O** with Fe^{3+} could be restored. Note that **1O′** also exhibited excellent fluorescent switching properties under alternate irradiations with UV/vis lights in aqueous acetonitrile (v/v = 1 : 1) (Fig. 3E). In the photostationary state, the fluorescence emission intensity was quenched 82% due to the formation of **1C′** with the

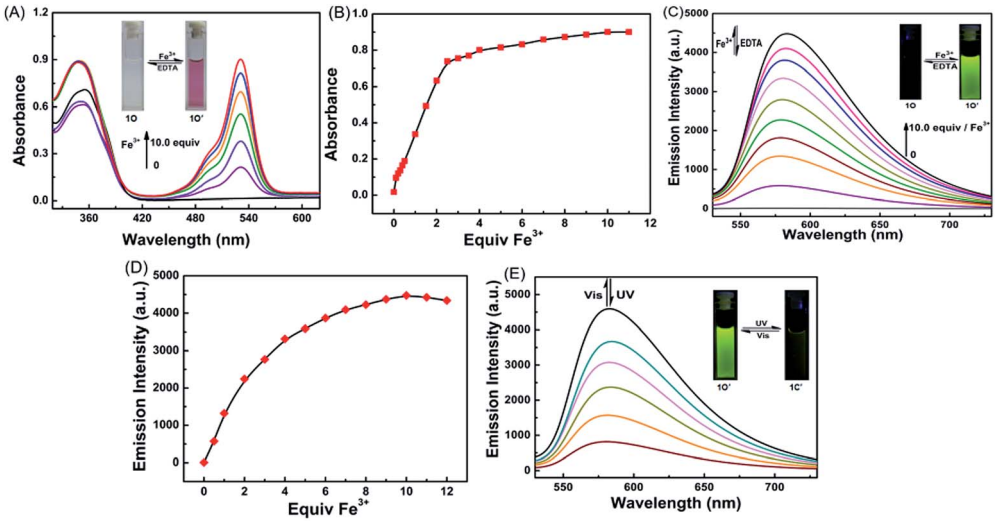

Fig. 3 (A) Fluorescence properties of **1O** in aqueous acetonitrile ($C = 2.0 \times 10^{-5}$ mol L^{-1}, v/v = 1 : 1, $\lambda_{ex} = 515$ nm) induced by Fe^{3+}/EDTA. (B) Upon addition of different equivalents of Fe^{3+} and the emission intensity curve at 585 nm. (C) The absorption spectra of **1O′** in aqueous acetonitrile ($C = 2.0 \times 10^{-5}$ mol L^{-1}, v/v = 1 : 1) induced by Fe^{3+}/EDTA. (D) The absorption intensity changes of **1O** at 531 nm with different equivalents of Fe^{3+}. (E) Changes in the fluorescence of **1O′** in aqueous acetonitrile ($C = 2.0 \times 10^{-5}$ mol L^{-1}, v/v = 1 : 1, $\lambda_{ex} = 515$ nm) upon alternating irradiation with UV/vis light.

fluorescence changing from bright green-yellow to dark yellow. These results indicate that the diarylethene derivative **1O** is a promising candidate for fluorescence-switching devices due to fluorescence switching behavior induced by both Fe^{3+}/EDTA and UV/vis light.

Job's plot analysis was conducted on the fluorescence titration data, as previously reported, to calculate the binding ratio between **1O** and Fe^{3+}.[34,35] As shown in Fig. 4A, the concentration of **1O′** reached a maximum as the molar fraction of $[Fe^{3+}]/([Fe^{3+}] + [\mathbf{1O}]) = 0.5$, indicating that the complex ratio between Fe^{3+} and **1O** was 1 : 1 in the aqueous acetonitrile solution (v/v = 1 : 1). The association constant (K_a) of **1O** with Fe^{3+} was determined to be 5.9793×10^4 mol L^{-1} by the Benesi–Hildebrand equation (Fig. 4B),[36] and the limit of detection of Fe^{3+} by **1O** was found to be 65 nM (3δ per slope) (Fig. 4C). These results indicate that **1O** is highly selective towards Fe^{3+} and can be used as a fluorescence sensor of Fe^{3+}.

The selectivity of a chemosensor towards the analyte over the other competitive species is a very important parameter to evaluate its sensing performance.[37] To further confirm the high selectivity of the **1O** sensor towards Fe^{3+}, competitive tests were conducted in the presence of metal ions with similar properties: Cd^{2+}, Ba^{2+}, Mg^{2+}, Ca^{2+}, Pb^{2+}, K^{+}, Co^{2+}, Zn^{2+}, Sr^{2+}, Mn^{2+}, Ni^{2+}, Al^{3+}, Cr^{3+}, Cu^{2+}, and Hg^{2+}. Fig. 5 shows the fluorescence response of **1O** to Fe^{3+} in the aqueous acetonitrile solution as different ions (20.0 equiv.) were added. No obvious interference was observed from other competitive metal ions in aqueous acetonitrile, indicating that **1O** was highly selective towards Fe^{3+}. The present sensor was compared with other sensors

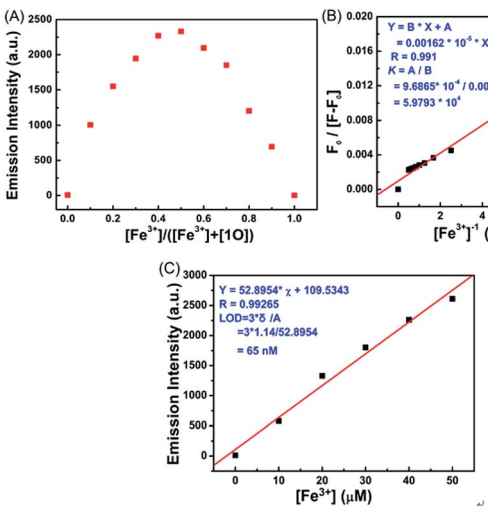

Fig. 4 (A) The Job's plot showing the 1 : 1 complex of **1O** and Fe^{3+}. (B) Hildebrand–Benesi plot based on the 1 : 1 ratio between **1O** and Fe^{3+}, the binding constant of **1O** with Fe^{3+} was calculated to be 5.9793×10^4 mol L^{-1}. (C) The limit of detection (LOD) is 65 nM.

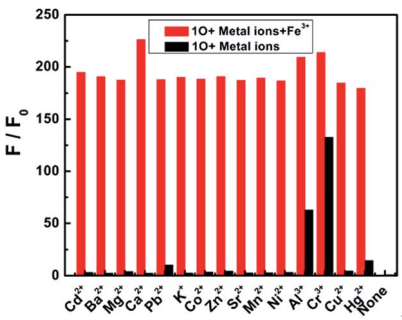

Fig. 5 Emission changes at 585 nm of **1O** in the presence of different metal ions added in the amount of 20.0 equiv. ($\lambda_{ex} = 515$ nm) in acetonitrile/water binary solvent ($C = 2.0 \times 10^{-5}$ mol L^{-1}, v/v = 1 : 1), after the initial addition of Fe^{3+} (10.0 equiv.) to the above solution.

reported for Fe^{3+} detection in recent years,[38–44] as listed in Table 1. These sensors showed some good physical properties such as lower LOD, association constant, high sensitivity and so on. For the **1O**–Fe^{3+} complex, a moderate performance in all aspects was observed, suggesting that diarylethene **1O** could serve as a fluorescence sensor for Fe^{3+}.

Acidichromism

It is particularly well-known that the open ring form of the rhodamine moiety in the presence of a proton emits strong fluorescence in the range of 540–700 nm.[45,46] As shown in Fig. 6A and Fig. S5,† the fluorescence intensity of **1O** ($C = 2.0 \times 10^{-5}$ mol L^{-1}) in acetonitrile at 595 nm under excitation at 515 nm was significantly enhanced by TFA due to the formation of an open ring fluorescent rhodamine moiety. The fluorescence intensity reached a maximum in the presence of 30 equiv. TFA and the absolute fluorescent quantum yield of the protonated **1O** (**1O″**) was determined to be 0.55. The addition of TEA to the **1O″** solution re-generated the spirolactam form of rhodamine. The fluorescent emission at 583 nm disappeared, and the bright green-yellow fluorescence of the solution diminished (Fig. 6A). Further addition of TFA produced the protonated **1O″**. As shown in Fig. 6B, the spirolactam form of **1O** was non-absorbing, whereas the open ring form exhibited a visible absorption band centered at 529 nm and the solution changed from colorless to pink, which could be easily observed with the naked eye. The absorption reached a maximum with 30.0 equiv. TFA and further increasing TFA equiv. caused no significant change in the absorption (Fig. S6†). The reversible modulation of fluorescent emission *via* alternating additions of TFA and TEA for 10 cycles resulted in no significant decrease in the emission intensity of **1O** (Fig. 6D).

Table 1 Comparative study of the analytical performance of **1O**–Fe^{3+} with other recently reported sensors

Sensor	Approaches	LOD	K_a	Ref.
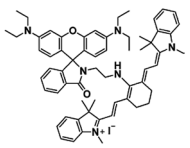	Fluorescence increase	737 nM	—	*Sens. Actuators B*, 2016, **224**, 661–667
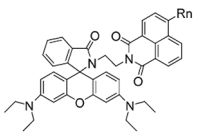	Fluorescence increase	418 nM	1.88×10^4	*J. Lumin.*, 2015, **157**, 143–148
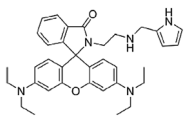	Fluorescence increase	31 nM	2.19×10^4	*Bioorg. Med. Chem.*, 2014, **22**, 4826–4835
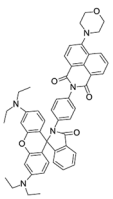	Fluorescence increase	105 nM	1.24×10^5	*Talanta*, 2014, **128**, 69–74
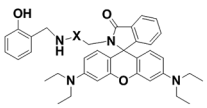	Fluorescence increase	2×10^4 nM	—	*Sens. Actuators B*, 2012, **174**, 231–236
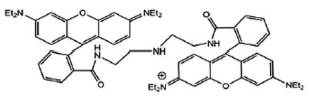	Fluorescence quenching	300 nM	—	*Talanta*, 2013, **106**, 261–265
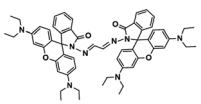	Fluorescence increase	1.1 nM	log() = 4.72 ± 0.27	*Sens. Actuators B*, 2013, **178**, 228–232
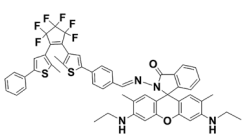	Fluorescence increase	65 nM	5.9793×10^4	This work

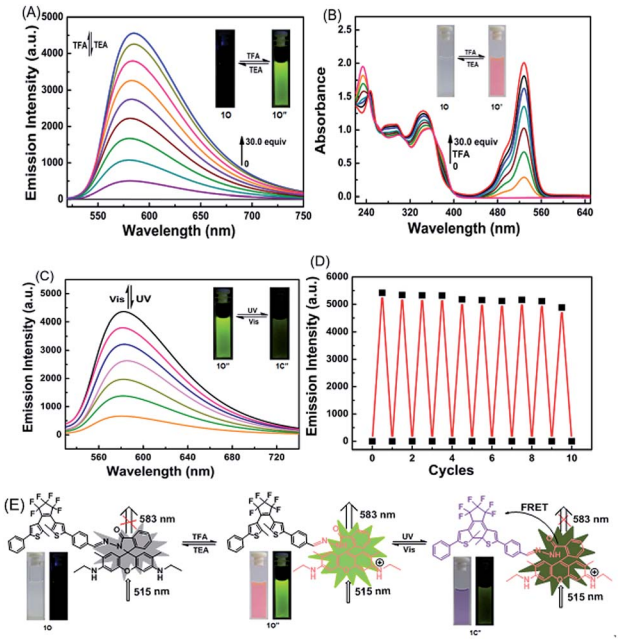

Fig. 6 (A) Fluorescence (λ_{ex} = 515 nm) change of **1O** in acetonitrile ($C = 2.0 \times 10^{-5}$ mol L^{-1}) induced by TFA/TEA. (B) Changes in absorption spectra of **1O″** in acetonitrile ($C = 2.0 \times 10^{-5}$ mol L^{-1}) induced by TFA/TEA. (C) Fluorescence (λ_{ex} = 515 nm) change of **1O″** upon alternating irradiation with UV/vis light. (D) Acid–base cycle of **1O** in acetonitrile ($C = 2.0 \times 10^{-5}$ mol L^{-1}) at room temperature. (E) Principle of reversible molecular switching and the color changes of **1O**.

As discussed above, the color of **1O″** solution could be changed *via* alternating irradiating with UV/vis lights. Based on this feature, it can be anticipated that the diarylethene derivatives bearing chemo-responsive function groups offer a promising approach to the design of optical molecular switches.[47,48] **1O″** in acetonitrile underwent a photocyclization reaction under irradiation at 297 nm, exhibiting a strong emission peak at 582 nm that significantly decreased with the isomerization from **1O″** to **1C″** under visible light irradiation (Fig. 6C). The fluorescence intensity of **1O″** decreased 85%, accompanied by the fluorescence change from bright green-yellow to dark at the photostationary state, which was a typical behaviour of the FRET mechanism. FRET usually occurs between the open ring rhodamine acylhydrazine (the donor) and the closed-ring diarylethene (the acceptor), resulting in intrinsic photoluminescence properties. The fluorescence color and emission spectrum of **1O″** can be restored *via* irradiation with visible light of λ > 500 nm. Fig. 6E shows the switching behavior of **1O** induced by the stimulations of proton and UV/vis lights. These results indicate that **1O** can be potentially used as a dual-control molecular switch by TFA/TEA and UV/vis light.

Application in a logic circuit

As discussed above, the emission intensity of diarylethene **1O** was successfully modulated by either UV/vis light or Fe^{3+}/EDTA stimuli in an aqueous acetonitrile solution (Fig. 7A). Based on this observation, a logic circuit was constructed by four inputs

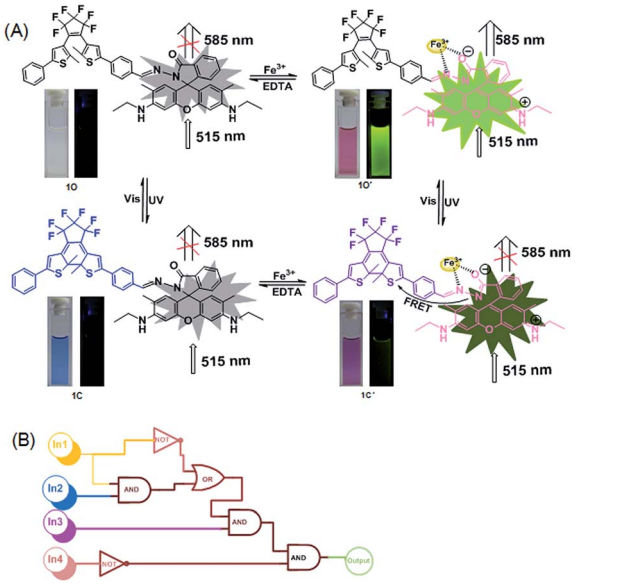

Fig. 7 (A) Dual-controlled fluorescent-switching behavior of **1O** induced by Fe^{3+}/EDTA and UV/vis light stimuli. (B) The combinational logic circuits equivalent to the truth table given in Table 1: In 1 (297 nm light), In 2 (λ > 500 nm light), In 3 (Fe^{3+}), In 4 (EDTA) and output (fluorescence at 585 nm).

including 297 nm UV light, visible light (λ > 500 nm), Fe^{3+}, and EDTA. The fluorescent emission intensity at 585 nm was set as the output. The output with the emission intensity at 585 nm higher than *ca.* 2500 was considered as the on state with a Boolean value of 1 and the emission intensity lower than *ca.* 2500 was regarded as the off state with a Boolean value of 0. As shown in Fig. 7B, the state can be either on (on = 1) or off (off = 0) with different Boolean values. For example, In 1 can be switched to the 'on' state with the Boolean value of 1 in response

Table 2 Truth table for all possible strings of four binary-input data and the corresponding output digit

Input				
In 1 (UV light)	In 2 (vis light)	In 3 (Fe^{3+})	In 4 (EDTA)	Output λ_{em} = 585 nm
0	0	0	0	0
1	0	0	0	0
0	1	0	0	0
0	0	1	0	1
0	0	0	1	0
1	1	0	0	0
1	0	1	0	0
1	0	0	1	0
0	1	1	0	1
0	1	0	1	0
0	0	1	1	0
1	1	1	0	1
1	1	0	1	0
1	0	1	1	0
0	1	1	1	0
1	1	1	1	0

to irradiation at 297 nm and In 2 can be switched on by the irradiation of appropriate visible light ($\lambda > 500$ nm). In 3 was 1 with the addition of Fe^{3+} and In 4 was 1 with the addition of EDTA. The output was on with the Boolean value of 1 under the stimuli of all four inputs. The fluorescent emission intensity at 585 nm below *ca.* 2500 was set as the initial state where the logic circuit was off. The input strings In 3 = 1, In1 = 0, In 2 = 0, and In 4 = 0 gave an output signal of 1 (on). Table 2 shows all possibilities of the logic strings of the four inputs.

Conclusions

In summary, a new diarylethene derivative bearing a rhodamine 6G unit was designed and synthesized. It exhibited highly selective and sensitive turn-on fluorescence and a color change response visible with the naked eye towards Fe^{3+} in aqueous acetonitrile. The Job's plot of experimental data reveals that a 1 : 1 stoichiometry is the most favorable binding mode between **1O** and Fe^{3+}. In addition, the fluorescent emission of the complex can be turned on/off by UV/vis lights irradiation. Based on these results, an integrated digital circuit was constructed with the fluorescent emission intensity at 585 nm as the output.

Acknowledgements

The authors are grateful for the financial support received from the National Natural Science Foundation of China (21662015, 21363009, 221362013, 51373072), the Project of Jiangxi Academic and Technological leaders (20142BCB22010), the Project of the Science Funds of the Jiangxi Education Office (KJLD13069), and the innovation fund of graduate students (YC2016-X02).

Notes and references

1 E. Erdema, N. Karapinarb and R. Donata, *J. Colloid Interface Sci.*, 2004, **280**, 309–314.
2 D. Wang, X. Y. Xiang, X. L. Yang, X. D. Wang, Y. L. Guo, W. S. Liu and W. W. Qin, *Sens. Actuators, B*, 2014, **201**, 246–254.
3 W. Sun, D. Y. Hu, Z. B. Wu, B. A. Song and S. Yang, *Chin. J. Org. Chem.*, 2011, **31**, 997–1010.
4 G. J. Park, I. H. Hwang, E. J. Song, H. Kim and C. Kim, *Tetrahedron*, 2014, **70**, 2822–2828.
5 K. Rurack, *Spectrochim. Acta, Part A*, 2001, **57**, 2161–2195.
6 J. F. Zhang, Y. Zhou, J. Yoon and J. S. Kim, *Chem. Soc. Rev.*, 2011, **40**, 3416–3429.
7 K. P. Carter, A. M. Young and A. E. Palmer, *Chem. Rev.*, 2014, **114**, 4564–4601.
8 P. S. Hardikar, S. M. Joshi, D. S. Bhat, D. A. Raut, P. A. Katre, H. G. Lubree and C. S. Yajnik, *Diabetes Care*, 2012, **35**, 797–802.
9 J. Comin-Colet, M. Lainscak, K. Dickstein, G. S. Filippatos, P. Johnson, T. F. Lüscher, C. Mori, R. Willenheimenr, P. Poniknowski and S. D. Anker, *Eur. Heart J.*, 2013, **34**, 30–38.
10 A. Malek, T. Thomas and E. Prasad, *ACS Sustainable Chem. Eng.*, 2016, **4**, 3497–3503.
11 T. Ganz, *Blood*, 2003, **102**, 783–788.
12 A. P. De Silva, H. Q. N. Gunaratne, T. Gunnlaugsson, A. J. Huxley, C. P. McCoy, J. T. Rademacher and T. E. Rice, *Chem. Rev.*, 1997, **97**, 1515–1566.
13 X. Y. Qu, Q. Liu, X. N. Ji, H. C. Chen, Z. K. Zhou and Z. Shen, *Chem. Commun.*, 2012, **48**, 4600–4602.
14 C. Wolf, X. Mei and H. K. Rokadia, *Tetrahedron Lett.*, 2004, **45**, 7867–7871.
15 J. Zhang, Q. Zou and H. Tian, *Adv. Mater.*, 2013, **25**, 378–399.
16 A. Toriumi, S. Kawata and M. Gu, *Opt. Lett.*, 1998, **23**, 1924–1926.
17 M. Irie, *Chem. Rev.*, 2000, **100**, 1685–1716.
18 K. Y. Liu, Y. Wen, T. Shi, Y. Li, F. Y. Li, Y. L. Zhao, C. H. Huang and T. Yi, *Chem. Commun.*, 2014, **50**, 9141–9144.
19 G. M. Liao, C. H. Zheng, D. D. Xue, C. B. Fan, G. Liu and S. Z. Pu, *RSC Adv.*, 2016, **6**, 34748–34753.
20 S. H. Jing, C. H. Zheng, S. Z. Pu, C. B. Fan and G. Liu, *Dyes Pigm.*, 2014, **107**, 38–44.
21 S. Pal, N. Chatterjee and P. K. Bharadwaj, *RSC Adv.*, 2014, **4**, 26585–26620.
22 X. Zeng, L. Dong, C. Wu, L. Mu, S. F. Xue and Z. Tao, *Sens. Actuators, B*, 2009, **141**, 506–510.
23 M. Morimoto and M. Irie, *Chem. Commun.*, 2005, **31**, 3895–3905.
24 S. Yamamoto, K. Matsuda and M. Irie, *Org. Lett.*, 2003, **5**, 1769–1772.
25 R. J. Wang, S. Z. Pu, G. Liu and S. Q. Cui, *Beilstein J. Org. Chem.*, 2012, **8**, 1018–1026.
26 Z. Wang, D. Wu, G. Wu, N. Yang and A. Wu, *J. Hazard. Mater.*, 2013, **244**, 621–627.
27 D. Wu, W. Huang, C. Duan, Z. Lin and Q. Meng, *Inorg. Chem.*, 2007, **46**, 1538–1540.
28 Z. X. Li, L. Y. Liao, W. Sun, C. H. Xu, C. Zhang, C. J. Fang and C. H. Yan, *J. Phys. Chem. C*, 2008, **112**, 5190–5196.
29 S. Kawai, T. Nakashima, K. Atsumi, T. Sakai, M. Harigai, Y. Imamoto and T. Kawai, *Chem. Mater.*, 2007, **19**, 3479–3483.
30 M. Morimoto and M. Irie, *Chem.–Eur. J.*, 2006, **12**, 4275–4282.
31 T. Nakashima, K. Miyamura, T. Sakai and T. Kawai, *Chem.–Eur. J.*, 2009, **15**, 1977–1984.
32 M. Irie, T. Lifka, S. Kobatake and N. Kato, *J. Am. Chem. Soc.*, 2000, **122**, 4871–4876.
33 M. J. Yuan, Y. L. Li, J. B. Li, C. H. Li, X. F. Liu, J. Lv, J. L. Xu, H. B. Liu, S. Wang and D. B. Zhu, *Org. Lett.*, 2007, **9**, 2313–2316.
34 X. B. Yang, B. X. Yang, J. F. Ge, Y. J. Xu, Q. F. Xu, J. Liang and J. M. Lu, *Org. Lett.*, 2011, **13**, 2710–2713.
35 R. Kato, S. Nishizawa, T. Hayashita and N. Teramae, *Tetrahedron Lett.*, 2001, **42**, 5053–5056.
36 H. A. Benesi and J. H. Hildebrand, *J. Am. Chem. Soc.*, 1949, **71**, 2703–2707.
37 M. Saleem and K. H. Lee, *RSC Adv.*, 2015, **5**, 72150–72287.
38 S. Li, D. Zhang, X. Y. Xie, S. G. Ma, Y. Liu, Z. H. Xu, Y. F. Gao and Y. Ye, *Sens. Actuators, B*, 2016, **224**, 661–667.

39 C. C. Wang, Y. Q. Liu, J. Y. Cheng, J. H. Song, Y. F. Zhao and Y. Ye, *J. Lumin.*, 2015, **157**, 143–148.
40 X. F. Bao, J. X. Shi, X. M. Nie, B. J. Zhou, X. L. Wang, L. Y. Zhang, H. Liao and T. Pang, *Bioorg. Med. Chem.*, 2014, **22**, 4826–4835.
41 C. C. Wang, D. Zhang, X. Y. Huang, P. G. Ding, Z. J. Wang, Y. F. Zhao and Y. Ye, *Talanta*, 2014, **128**, 69–74.
42 M. M. Chai, D. Zhang, M. Wang, H. J. Hong, Y. Ye and Y. F. Zhao, *Sens. Actuators, B*, 2012, **174**, 231–236.
43 Y. Y. Du, M. Chen, Y. X. Zhang, F. Luo, C. Y. He, M. J. Li and X. Chen, *Talanta*, 2013, **106**, 261–265.
44 V. Bhalla, N. Sharma, N. Kumar and M. Kumar, *Sens. Actuators, B*, 2013, **178**, 228–232.
45 K. Ghosh, T. Sarkar, A. Majumdar, S. K. Mandal and A. R. Khuda-Bukhsh, *Anal. Methods*, 2014, **6**, 2648–2654.
46 S. J. Lim, J. Seo and S. Y. Park, *J. Am. Chem. Soc.*, 2006, **128**, 14542–14547.
47 L. N. Lucas, J. J. D. de Jong, J. H. Van Esch, R. M. Kellogg and B. L. Feringa, *Eur. J. Org. Chem.*, 2003, **2003**, 155–166.
48 W. R. Algar, M. Massey and U. J. Krull, *TrAC, Trends Anal. Chem.*, 2009, **28**, 292–306.